

To verify that the Au is actually alloyed into the first layer of the Ni catalyst, we examined the structure and composition of the active catalyst by extended x-ray absorption fine structure spectroscopy (EXAFS). The EXAFS spectrum of the bimetallic catalyst was recorded in situ under synthesis conditions to make sure it is the active catalyst that is studied (Fig. 4). Only if we allow for the possibility that Au atoms have Ni neighbors at Ni interatomic distances can we account for the spectrum. Because Au is immiscible in bulk Ni, this demonstrates that Au is alloyed into the Ni surface layer as on the single crystal model systems.

The steam-reforming activity was measured for the Ni catalyst and for the Au/Ni catalyst for which the EXAFS data are recorded (Fig. 5). The only difference between the two samples is in the Au modification. Both samples were first reduced in pure H and subsequently exposed to a diluted *n*-butane gas at 550°C. We used *n*-butane to test the activity because it gives rise to the most severe graphite formation problems. The *n*-butane conversion as a function of time on stream starts out at about 99.99%. It is seen that the pure Ni catalyst deactivates rapidly, whereas the conversion for the Au/Ni sample is almost constant. The deactivation is typical of a Ni catalyst under these extreme conditions, and it can be associated with the formation of graphite as seen in, for example, electron microscopy. The Au-containing sample, in contrast, does not produce graphite. This has been checked by independent thermogravimetric measurements.

In conclusion, we are approaching a point where fundamental insight into surface structure and reactivity can be applied directly to the design of new catalysts. By combining several experimental surface science techniques with theory and insight into synthesis and in situ characterization of high surface area catalysts, it has been possible to go beyond our fundamental understanding of the atomic processes involved in catalysis to the design of an improved catalyst for the steam-reforming reaction.

#### REFERENCES AND NOTES

1. G. Ertl, in *Catalytic Ammonia Synthesis*, J. R. Jennings, Ed. (Plenum, New York, 1991), p. 109; D. R. Strongin and G. A. Somorjai, in *ibid.*, p. 1; D. W. Goodman, R. D. Kelly, T. E. Madey, J. T. Yates Jr., *J. Catal.* **63**, 226 (1980); J. Yoshihara and C. T. Campbell, *ibid.* **161**, 776 (1996); G. A. Papapolymerou and L. D. Schmidt, *Langmuir* **1**, 488 (1985); V. P. Zhdanov and B. Kasemo, *Surf. Sci. Rep.* **20**, 111 (1996); S. H. Oh, G. B. Fisher, J. E. Carpenter, D. W. Goodman, *J. Catal.* **100**, 360 (1986).
2. D. A. King, *Stud. Surf. Sci. Catal.* **109**, 79 (1997); J. M. Bradley, A. Hopkinson, D. A. King, *J. Phys. Chem.* **99**, 17032 (1995).
3. J. Rostrup-Nielsen, in *Catalysis, Science and Technology*, J. R. Anderson and M. Boudart, Eds. (Springer, Berlin, 1984), vol. 5, p. 1.

4. ———, *J. Catal.* **85**, 31 (1984); N. T. Andersen, F. Topsoe, I. Alstrup, J. Rostrup-Nielsen, *ibid.* **104**, 454 (1987).
5. J. H. Sinfelt, *Bimetallic Catalysts: Discoveries, Concepts, and Applications* (Wiley, New York, 1983); V. Ponec, *Adv. Catal.* **32**, 149 (1983).
6. G. A. Attard and D. A. King, *Surf. Sci.* **188**, 589 (1987); F. Besenbacher, L. Pleth Nielsen, P. T. Sprunger, in *The Chemical Physics of Solid Surfaces and Heterogeneous Catalysis*, D. A. King and D. P. Woodruff, Eds. (Elsevier, Amsterdam, 1997), vol. 8, chap. 10.
7. L. Pleth Nielsen *et al.*, *Phys. Rev. Lett.* **71**, 754 (1993).
8. M. B. Lee, Q. Y. Yang, S. T. Ceyer, *J. Chem. Phys.* **87**, 2724 (1987).
9. P. Kratzer, B. Hammer, J. K. Nørskov, *ibid.* **105**, 5595 (1996).
10. O. Swang, J. K. Faegri, O. Gropen, U. Wahlgren, P. E. M. Siegbahn, *Chem. Phys.* **156**, 379 (1991); H. Yang and J. L. Whitten, *J. Chem. Phys.* **96**, 5529 (1992); H. Burghgraef, A. P. J. Jansen, R. A. van Santen, *ibid.* **101**, 11012 (1994).
11. T. P. Beebe Jr., D. W. Goodman, B. D. Kay, J. T. Yates, *J. Chem. Phys.* **87**, 2305 (1987); P. M. Holmblad, J. Wambach, I. Chorkendorff, *ibid.* **102**, 8255 (1995).
12. B. Hammer and J. K. Nørskov, *Nature* **376**, 238 (1995).
13. P. M. Holmblad, J. Hvolbæk Larsen, I. Chorkendorff, *J. Chem. Phys.* **104**, 7289 (1996).
14. P. M. Holmblad *et al.*, *Catal. Lett.* **40**, 131 (1996).
15. The calculation is done selfconsistently with ultrasoft pseudopotentials, a slab of three metal layers, and plane waves with kinetic energies up to 25 rydberg at 54 k-points in the first Brillouin zone. Relaxation of the C and the metal atoms in the outermost surface layer is included. Exchange and correlation effects are described within the generalized gradient approximation of J. P. Perdew *et al.* [*Phys. Rev. B* **46**, 6671 (1992)].
16. We gratefully acknowledge the important preparative work by J. Hyltoft as well as help and suggestions from I. Alstrup and J. Rostrup-Nielsen. The present work was financed in part by the Danish Research Councils through the Center for Surface Reactivity, DANSYNC, and grant 9501775. We also thank Hasylab for offering beamtime at the ROEMO II EXAFS spectrometer. The Center for Atomic-scale Materials Physics (CAMP) is sponsored by the Danish National Research Foundation. A patent application describing the use of Au/Ni as a steam-reforming catalyst has been submitted [DK patent application 0683/97 (1997)].

26 November 1997; accepted 19 January 1998

## The Theropod Ancestry of Birds: New Evidence from the Late Cretaceous of Madagascar

Catherine A. Forster,\* Scott D. Sampson, Luis M. Chiappe, David W. Krause

A partial skeleton of a primitive bird, *Rahona ostromi*, gen. et sp. nov., has been discovered from the Late Cretaceous of Madagascar. This specimen, although exhibiting avian features such as a reversed hallux and ulnar papillae, retains characteristics that indicate a theropod ancestry, including a pubic foot and hyposphene-hypantra vertebral articulations. *Rahona* has a robust, hyperextendible second digit on the hind foot that terminates in a sicklelike claw, a unique characteristic of the theropod groups Troodontidae and Dromaeosauridae. A phylogenetic analysis places *Rahona* with *Archaeopteryx*, making *Rahona* one of the most primitive birds yet discovered.

The origin of birds has been debated for more than 100 years, with theropod dinosaurs (1–6) and basal archosauriforms (7, 8) most frequently hypothesized as their ancestors. Several workers have argued explicitly against the “birds as dinosaurs” theory (8–12). We report here a new raven-sized primitive bird that adds new morphological data to the question of bird ancestry. The holotype specimen of this new bird, *Rahona ostromi*, gen. et sp. nov. (13), was recovered from a small quarry (site MAD93-18) in Upper Cretaceous rocks in northwestern

Madagascar. This quarry has produced a diverse, well-preserved vertebrate fauna, including the primitive bird *Vorona berivotrensis* (14).

The skeleton of *Rahona* exhibits a striking mosaic of theropod and derived avian features (Fig. 1). The specimen appears to be adult, based on the complete fusion of neural arches to vertebral centra (Fig. 2). The single camellate cervicodorsal vertebra bears a large hypophysis and bilateral pneumatic foramina, as in maniraptorans and birds, as well as a large vertebral canal (88% of the centrum height; Fig. 2B). Pneumatic foramina also occur on the dorsal vertebrae, lying within well-developed pneumatic fossae, as in some enantiornithines (Fig. 2A). The vertebral canals are large (42 to 62% of the centrum height), as in birds. The dorsal vertebrae have accessory hyposphene-hypantra articulations, a unique character of theropod and sauropod dinosaurs, retained only in *Patagonykus* (15)

C. A. Forster and D. W. Krause, Department of Anatomical Sciences, State University of New York at Stony Brook, Stony Brook, NY 11794, USA.

S. D. Sampson, Department of Anatomy, New York College of Osteopathic Medicine, Old Westbury, NY 11568, USA.

L. M. Chiappe, Department of Ornithology, American Museum of Natural History, 79th Street at Central Park West, New York, NY 10024, USA.

\*To whom correspondence should be addressed. E-mail: cforster@mail.som.sunysb.edu

among birds. There are six sacral vertebrae, one more than in most theropods and *Archaeopteryx*. They are completely co-ossified into an avianlike synsacrum (Fig. 2C). Like *Archaeopteryx*, *Rahona* retains a long bony tail. Thirteen caudal vertebrae (Cd) are preserved, but the complete number is unknown (Fig. 2D). The transition point is

proximally placed at Cd9.

The antebrachium of *Rahona* is avian; it is elongate (the ulna is 150% of the length of the femur), and the radius is reduced to 50% of the diameter of the ulna (Fig. 3, B and C and measurements in Table 1). The caudal (anconal) margin of the bowed ulna bears six low, slightly elongate papillae that

become less distinct distally (Fig. 3D). We interpret these to be quill knobs for the attachment of secondary flight feathers. These six quill knobs, which are regularly spaced (1.6 cm apart), cover only a portion of the ulnar shaft. We estimate that there is space for four additional feathers, for a total of approximately 10 secondary remiges,

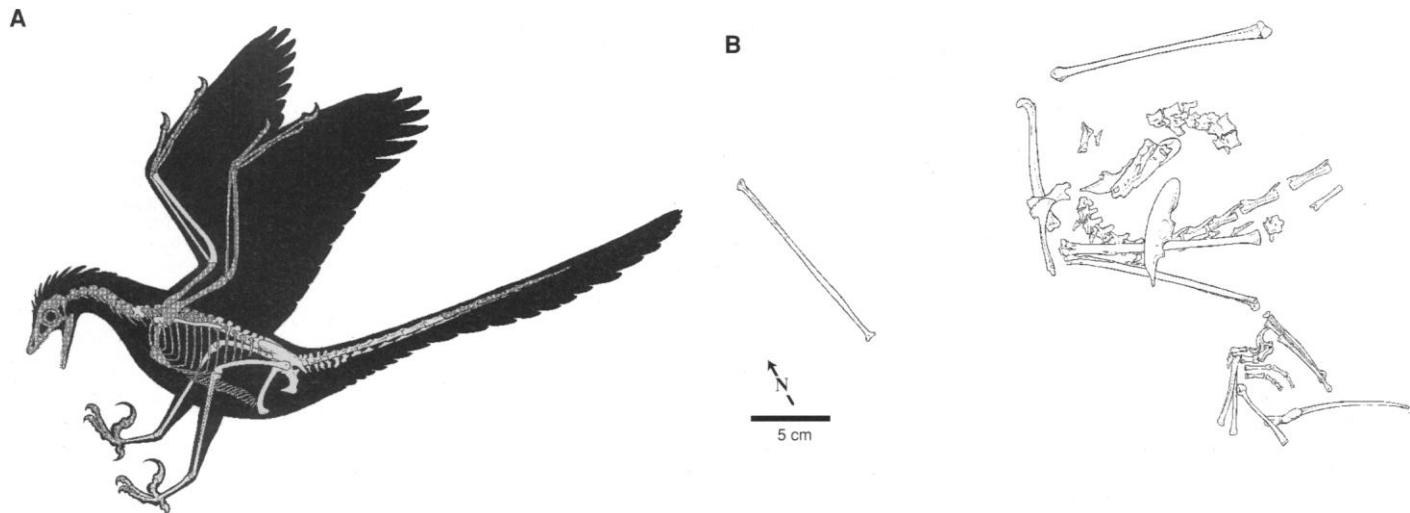


**Fig. 1.** *Rahona ostromi*, a new primitive bird from the Late Cretaceous of Madagascar. **(A)** Reconstruction in left lateral view, with missing elements indicated by shading. **(B)** Skeleton of *Rahona* as found in situ. The specimen is lying on its right side with its axial column in dorsiflexion. Almost all elements of the skeleton were discovered within an area of 500 cm<sup>2</sup>; most are pristinely preserved. Most preserved parts of the axial column (the last 6 dorsal, the synsacral, and the first 12 caudal vertebrae and chevrons) were found in virtually direct articulation. A 13th caudal vertebra and two chevrons were found closely behind the 12th caudal vertebra. A cervicodorsal vertebra

was found 5 cm in front of the dorsal series and, although isolated, was oriented and spaced as if in articulation with them. The pelvic elements were found either articulated with the synsacrum (right ilium) or in close proximity. The right hind limb, with the femur slightly displaced from the acetabulum, is closely articulated, but digits are missing from the pes. The lower left hind limb is loosely articulated (the femur was displaced approximately 1 m to the north) but has an articulated and nearly complete pes. The left scapula and right ulna were found touching or close to the rest of the bones; the right radius was displaced approximately 15 cm to the west. Scale bar = 5 cm.

**Fig. 2 (left).** Axial skeleton of *Rahona ostromi*. **(A)** Last six dorsal vertebrae in right lateral view. **(B)** Cervicodorsal vertebra in right lateral view. **(C)** Synsacrum in left lateral view. **(D)** Caudal vertebrae and articulated chevrons in left lateral view. Cd1 through Cd9 are on the top row and Cd 10 through Cd13 are on the bottom row. Abbreviation: h, hyposphene-hypantra articulation. Scale bars = 1 cm.

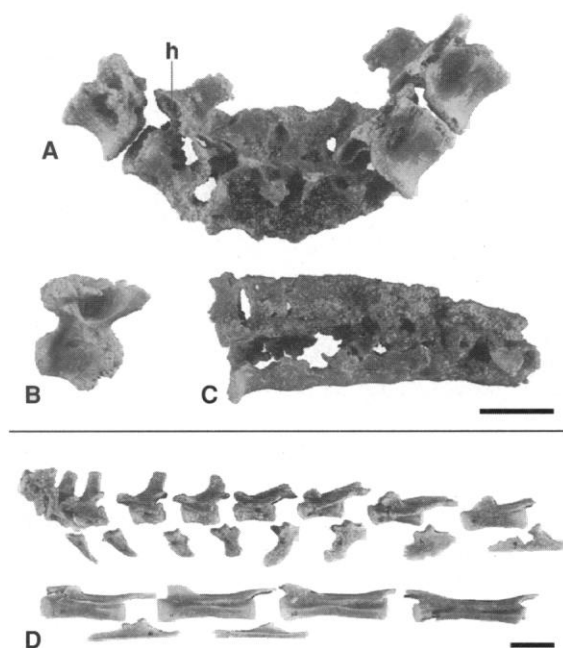
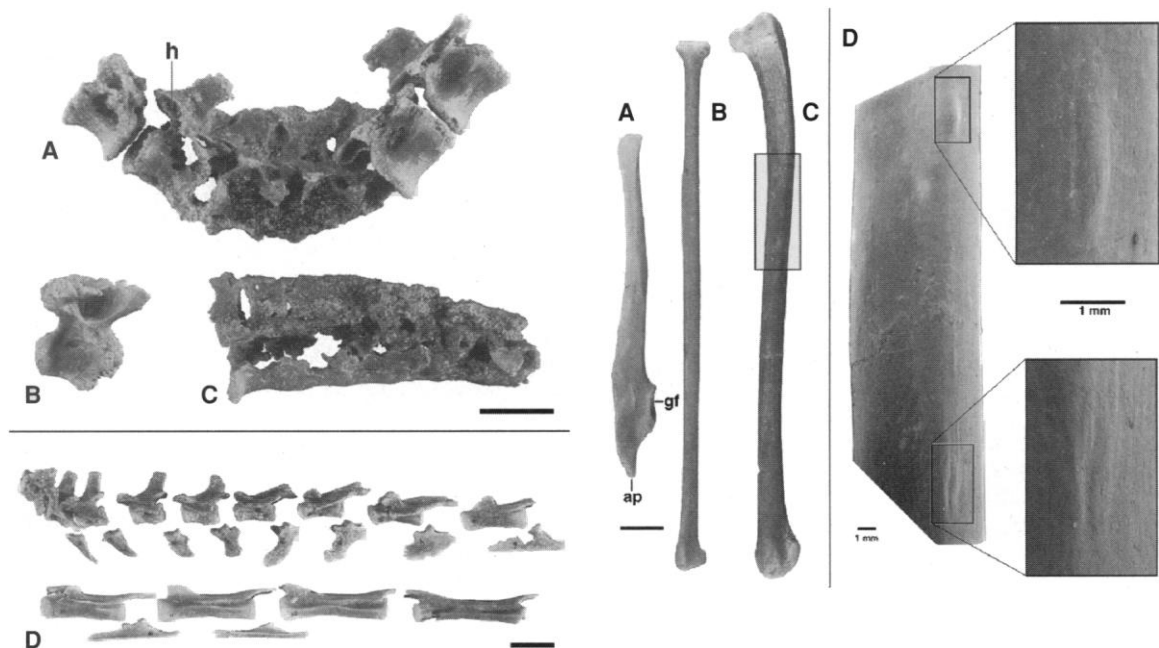


**Fig. 3 (right).** Wing elements of *Rahona ostromi*. **(A)** Left scapula in lateral view, caudal end up. **(B)** Right radius in cranial view, proximal end up. **(C)** Right ulna in medial view, proximal end up. The box indicates the limits of the scanning electron microscope photo shown in (D). **(D)** Scanning electron microscope photo of papillae on right ulna (left), with magnified views of two of the papillae (right). We interpret these as quill knobs. Abbreviations: ap, acromion process; gf, glenoid fossa. Scale bar for (A), (B), and (C) = 1 cm.



which is fewer than the 12 to 14 secondaries suggested for *Archaeopteryx* (16) but within the range known for extant birds.

The main axis of the glenoid fossa is centered on the ventral edge of the scapular blade, as in *Archaeopteryx* and theropods, rather than lateral to the ventral edge as in *Neornithes* (Fig. 3A). Otherwise, the scapula is quite derived. It has a facet for the coracoid, indicating a mobile joint as in derived birds, rather than the plesiomorphic sutural contact of theropods and *Archaeopteryx*. A well-developed acromion process projects well cranial to the coracoid facet, as in *Unenlagia*, *Archaeopteryx*, and birds. On the basis of these forelimb characters (enlarged acromion process, coracoid facet, elongate ulna, and ulnar papillae), the scapula of *Rahona* was probably positioned dorsally on the ribcage rather than more ventrally as in theropods, resulting in a more laterally directed glenoid fossa. This orientation allows for the more extensive vertical excursion of the humerus needed to produce a flight stroke (17) and contributes to the wing-folding mechanism (18).

The pelvic elements of *Rahona* closely resemble those of *Archaeopteryx* and *Unenlagia* (18). The ilium has a long preacetabular process (55% of the ilium length) and a short postacetabular process that is drawn back into a narrow, pointed posterior end. The pubis (90% of the ilium length) is oriented vertically (as in some maniraptorans, *Archaeopteryx*, and *Unenlagia*). Distally, the pubis sweeps caudally and expands into a foot; a well-developed hypopubic cup is present (Fig. 4A). A pubic foot is absent in nearly all avians, but is present in theropods, *Archaeopteryx*, *Patagonykus*, and enantiornithines (for example, *Sinornis* and *Cathayornis*). Like that of *Archaeopteryx*, the ischium of *Rahona* is short (45% of the length of the pubis), platelike, and has a pointed process at the anterodistal end (Fig. 4A). We interpret the latter as the obturator process, based on its shape and position. Behind the iliac articulation is a small dorsally projecting process [the "proximodorsal process" of Novas and Puerta (18)], a character shared exclusively with *Unenlagia* and the primitive birds *Archaeopteryx*, enantiornithines, *Iberomesornis*, and *Confuciusornis*. A second, smaller process is midway down the caudal ischial margin, as in *Archaeopteryx* and *Confuciusornis*. There is no evidence of an ischial symphysis. All pelvic elements are unfused, a plesiomorphic character state shared with nonavian theropods, *Archaeopteryx*, *Unenlagia*, and *Iberomesornis*.

The femoral head is identical to that of *Archaeopteryx*, lacking both a neck and a fossa for the capital ligament. It also bears an avianlike undivided trochanteric crest (Fig. 4B). The tibia is long and straight

(137% of the femoral length) and lacks a medial cnemial crest as occurs in more derived ornithurine birds. The greatly reduced, splintlike fibula is birdlike in proportion (15% of the tibial diameter), and the tubercle for the m. iliofibularis faces posteriorly, as in *Ornithurae* (Fig. 4C). The right fibula is preserved in articulation with the tibia, and its distal portion shifts onto the cranial surface of the tibia. If this is its natural position (as in *Patagopteryx*), it could not have articulated with the calcaneum. Loss of contact between the fibula and calcaneum characterizes birds.

The much reduced calcaneum is tucked into the lateral margin of the broad short astragalus (14% of tibial length), as in maniraptorans and *Archaeopteryx*. The astragalus and calcaneum are partially fused to one another but are not fused to the tibia (Fig. 4C). A free distal tarsal caps the right metatarsal IV. Plesiomorphic free tarsals are also retained in the primitive bird *Iberomesornis* and in some specimens of *Archaeopteryx*.

The foot of *Rahona* is primitive in many respects; notably the metatarsals are not fused to one another (Fig. 4D). In some specimens of *Archaeopteryx*, the metatarsals also lack any fusion (for example, the Eichstätt specimen), although other specimens exhibit partial fusion of the proximal metatarsals (for example, the London specimen). The digits of the left foot of *Rahona* were found in articulation and show that digit I is reversed relative to the other digits (Fig. 1B), a configuration known only in birds (10).

The most striking feature in the nearly complete left foot, however, is the structure of digit II. It is extremely robust relative to the other digits (the first phalanx of digit II is 140% of the width of that of digit III at midshaft) and distinctive in morphology. The phalanges have large, ventrolaterally placed flexor keels, expansive distal exten-

sor surfaces, and deep, dorsally placed, collateral ligament pits. The digit ends in an enlarged sickle-shaped claw. Although unguals are missing from digits III and IV, their preserved distal phalanges indicate that they bore substantially smaller claws. On the left foot, digit II was found in hyperextension, whereas digits III and IV were flexed (Fig. 1B). This distinctive morphology of an enlarged hyperextendible digit II is found only in dromaeosaurid and troodontid maniraptorans (for example, *Deinonychus*, *Velociraptor*, and *Troodon*), resulting in the predatory "slashing" foot (19).

The general skeletal morphology of *Rahona* is birdlike. *Rahona* is only slightly larger than the London *Archaeopteryx* specimen (though smaller than its avian contemporary *Vorona*) and extremely lightly built (the long bones are hollowed

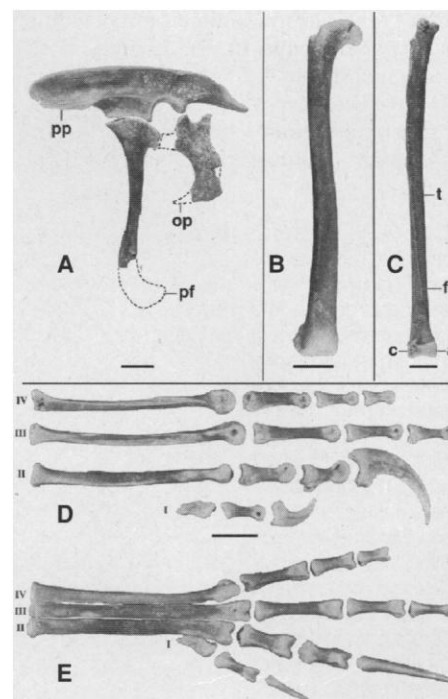


**Fig. 4.** Pelvis and hind limb of *Rahona ostromi*. (A) Left pelvis in lateral view. The ilium is complete; the pubis is missing its distal end; and the ischium is missing its obturator process, ischial articulation, and part of a small process in the middle of its caudal margin. These missing portions are present on the right pubis and ischium, and their outlines are indicated here by dotted lines. (B) Right femur in anterior view. (C) Right tibia, fibula, and proximal tarsals in anterior view. The proximal ends of the crural elements are slightly eroded but are complete on the left tibia and fibula. (D) Left pes in exploded medial view. (E) Articulated left pes in dorsal view. The ungual of digit III and the distal phalanx and ungual of digit IV are missing. Abbreviations: a, astragalus; c, calcaneum; f, fibula; op, obturator process; pf, pubic foot; pp, preacetabular process; t, tibia. Roman numerals refer to digit numbers. Scale bars = 1 cm.

**Table 1.** Lengths (in millimeters) of pelvic and limb elements of *Rahona ostromi*. Dash indicates that measurement is not possible because of an absent or incomplete element.

Element	Left	Right
Synsacrum		41.9
Scapula	82.2	—
Radius	—	126.9
Ulna	—	132.3
Ilium	66.7	67.7
Pubis	—	60.8
Ischium	27.3	—
Femur	88.0	87.1
Tibia	119.8	120.2
Fibula	—	—
Metatarsal I	8.9	—
Metatarsal II	44.7	44.1
Metatarsal III	48.0	48.1
Metatarsal IV	45.3	47.7

to the same degree seen in other birds). These factors, combined with the elongate feathered ulna and raptorial slashing foot, suggest that this bird was lightweight, active, predatory, and capable of powered flight. The combination of derived wing morphologies with a vertically oriented pubis in *Rahona* counters the recent suggestion that the development of an avian-style lung ventilation system suitable for the high metabolic demands of flight was coupled with a fully retroverted pubis (11). The vertical pubis of *Rahona* also bears a well-developed hypopubic cup, a morphology associated with suprapubic musculature and avian-style lung ventilation (11). *Rahona* thus shows that a hypopubic cup and opisthopuby did not develop in concert.

It has been hypothesized that birds belong to a derived clade of theropods called Maniraptora (2–5). However, the arrangement of taxa within Maniraptora, including exactly where birds fit, is debated. Both Dromaeosauridae (4, 5) and Troodontidae (20) have been hypothesized to be the closest relatives of birds.

We ran a phylogenetic analysis (21)

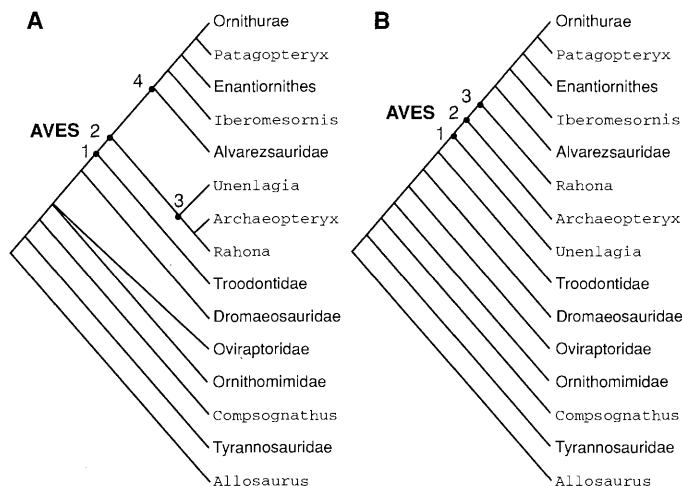
with two separate data sets, one including and one excluding forelimb elements for *Rahona* (22). The most parsimonious tree for both data sets shows the same arrangement of taxa within Aves (which includes *Rahona*). That is, the exclusion from the phylogenetic analysis of the strongly avian forelimb assigned to *Rahona* does not alter its phylogenetic position within Aves. *Rahona* is supported as a member of Aves [Avialae of others; for example, (3, 5)] by seven unambiguous derived characters; bootstrapping of the data set (500 replications) shows a 90% confidence level for our Aves node (Fig. 5A; the analyses depicted include forelimb characters for *Rahona*).

Our most parsimonious analysis places the purported maniraptoran theropod *Unenlagia* within Aves as the sister taxon to a *Rahona*-*Archaeopteryx* clade (Fig. 5A). This three-taxon clade is united by four unambiguous characters of the pelvis and femur (node 3 in Fig. 5A). Uniting these three taxa in a single subclade places them on a side branch of early bird evolution and supports the suggestion that *Archaeopteryx* was not a direct precursor of modern birds (12, 23). However, this clade collapses to a

paraphyletic configuration of (in order) *Unenlagia*-*Archaeopteryx*-*Rahona*-other birds, or *Archaeopteryx*-*Unenlagia*-*Rahona*-other birds, with only one additional step (see Fig. 5B for one of these trees). This suggests that the characters uniting these taxa may represent primitive features for birds rather than synapomorphies of a separate primitive bird lineage. These alternative hypotheses may prove more tenable, as *Rahona* shares a number of characters with more derived birds exclusive of *Archaeopteryx* (for example, six fused sacral vertebrae, a mobile scapulocoracoid joint, and an undivided trochanteric crest). *Rahona* remains firmly nested within Aves in all trees.

In addition to its numerous bird features (for example, a reversed hallux, a splintlike fibula, and ulnar papillae), *Rahona* retains specific theropod synapomorphies. The accessory hyposphene-hypantra articulations on its dorsal vertebrae are a synapomorphy of Saurischia (Sauropodomorpha + Theropoda) and are unknown in any other amniote clade (24). The singular pedal morphology is known only in derived maniraptoran theropods, which are the purported precursors of birds (25). Thus, the combination of morphological characters found in *Rahona* strongly supports its membership in Aves, as well as its theropod ancestry, and thus the dinosaurian origin of birds.

**Fig. 5. (A)** Phylogenetic hypothesis of relationships of *Rahona* to theropods and birds (this is a strict consensus tree of our two most parsimonious trees). Unambiguous synapomorphies distributed at each labeled node are as follows. Node 1 (Troodontidae + Aves): contact lost between distal ischia. Node 2 (Aves): teeth only slightly laterally compressed and nearly conical, loss of separate coronoid bone, number of caudal vertebrae reduced to 20 to 25, loss of pneumatic foramen on sacral vertebrae, ulnar distal condyle subtriangular in distal view and twisted more than 54° with respect to the proximal end, midshaft diameter of fibula reduced to one-fifth or less that of the tibia, and loss of deep fossa on the medial side of the proximal fibula. Node 3 (*Unenlagia* + *Archaeopteryx* + *Rahona*): preacetabular process of ilium twice as long as postacetabular process, postacetabular process shallow (less than 50% of the depth at the acetabulum) and drawn back into a pointed process, pubic foot projects caudally only, and loss of femoral neck. Node 4 (Metornithes): loss of jugular postorbital process, medial otic process of quadrate articulates with the prootic, ventral tubercle of humerus projects caudally and is separated from the humeral head by distinct capital incision, carpo-metacarpus present, prominent antitrochanter on ilium, loss of pubic foot, obturator process on ischium rudimentary or absent, and pubic apron transversely narrowed with pubic symphysis restricted to distal one-third of shaft. **(B)** Alternative phylogenetic hypothesis of one more step than that shown in (A). An *Archaeopteryx*-*Unenlagia*-*Rahona* arrangement is equally parsimonious but is not depicted here. Unambiguous synapomorphies distributed at each labeled node are as follows. Node 1: pubic foot projects caudally only. Node 2: teeth only slightly laterally compressed and nearly conical, loss of separate coronoid bone, number of caudal vertebrae reduced to 20 to 25, loss of pneumatic foramina on sacral vertebrae, ulnar distal condyle subtriangular in distal view and twisted more than 54° with respect to the proximal end, and midshaft diameter of fibula reduced to one-fifth or less that of the tibia. Node 3: ratio of height of neural canal in dorsal vertebrae to height of cranial articular face more than 0.40, undivided trochanteric crest, deep fossa on medial side of fibula absent, and fibula does not reach tarsus.



## REFERENCES AND NOTES

1. E. D. Cope, *Proc. Acad. Nat. Sci. Phila.* **1867**, 234 (1867); T. H. Huxley, *Geol. Mag.* **5**, 357 (1868); S. W. Williston, *Kans. City Rev. Sci.* **3**, 457 (1879); L. Witmer, in *Origin of the Higher Groups of Tetrapods*, H.-P. Schultze and L. Trueb, Eds. (Comstock, Ithaca, NY, 1991), pp. 427–466; P. C. Sereno and C. Rao, *Science* **255**, 845 (1992); L. M. Chiappe, *Nature* **378**, 349 (1995). To increase readability and conserve space, we use the shorthand terms "theropod" and "maniraptoran" in place of "nonavian theropod" and "nonavian maniraptoran," respectively.
2. J. H. Ostrom, *Biol. J. Linn. Soc.* **8**, 91 (1976).
3. J. A. Gauthier, *Mem. Calif. Acad. Sci.* **8**, 1 (1986).
4. T. R. Holtz Jr., *J. Paleontol.* **68**, 1100 (1994).
5. F. E. Novas, *Mem. Queensl. Mus.* **39**, 675 (1996).
6. L. M. Chiappe, *ibid.*, p. 533.
7. G. Heilmann, *The Origin of Birds* (Appleton, New York, 1927); A. S. Romer, *Vertebrate Paleontology* (Univ. of Chicago Press, Chicago, IL, 1966); P. Brodkorb, in *Avian Biology*, D. S. Farner, J. R. King, K. C. Parkes, Eds. (Academic Press, New York, 1971), pp. 19–55.
8. S. Tarsitano, in *Origin of the Higher Groups of Tetrapods*, H.-P. Schultze and L. Trueb, Eds. (Comstock, Ithaca, NY, 1991), pp. 541–576.
9. A. Feduccia and R. Wild, *Naturwissenschaften* **80**, 564 (1993); A. C. Burke and A. Feduccia, *Science* **278**, 666 (1997).
10. A. Feduccia and L. Martin, *Mus. North Ariz. Bull.* **60**, 185 (1996).
11. J. A. Ruben et al. *Science* **278**, 1267 (1997).
12. L. D. Martin, in *Origin of the Higher Groups of Tetrapods*, H.-P. Schultze and L. Trueb, Eds. (Comstock, Ithaca, NY, 1991), pp. 485–540.
13. The holotype specimen of *Rahona ostromi* is cataloged as Université d'Antananarivo (UA) 8656. Locality: MAD93-18, Upper Cretaceous (?Campanian) Maevarano Formation, Mahajanga Basin, northwestern Madagascar; collected by a joint expedition of the State University of New York at Stony Brook

- and the Université d'Antananarivo in 1995. Etymology: *Rahona* (RAH-hoo-nah; Malagasy): meaning menace/threat or cloud; intended interpretation: "menace from the clouds"; *ostromi*: in honor of Dr. John H. Ostrom. Diagnosis: *Rahona ostromi* is distinguished from all other avians by retention of a robust, hyperextendible, pedal digit II; from all other avians except *Patagonykus* by hyposphene-hypantra articulations on dorsal vertebrae; from *Archaeopteryx* by six fused sacral vertebrae and a greatly reduced fibula lacking contact with the calcaneum; from nonavian theropods, *Archaeopteryx*, and alvarezsaurids by its relatively elongate ulna with ulnar papillae and mobile scapulocoracoid articulation; from all other avians except *Archaeopteryx* and alvarezsaurids by retention of a long tail lacking a pygostyle; and from nonavian theropods by neural canals at least 40% of the height of the dorsal vertebral centra, proximal tibia of equal width and length, lack of a medial fossa on the fibula, and a reversed pedal digit I.
14. C. A. Forster *et al.*, *Nature* **382**, 532 (1996).
  15. The placement of *Patagonykus* and other alvarezsaurids (*Mononykus* and *Alvarezsaurus*) within Aves, although supported by cladistic analyses [for example, see (5, 6) and this analysis], is questioned by other researchers (10). Elimination of Alvarezsauridae from the phylogenetic analyses presented in this report does not alter the placement of *Rahona* within Aves.
  16. B. Stephan, *Urvögel Archaeopterygiformes* (Ziemen, Wittenberg, Germany, 1974); S. Rietschel, in *The Beginnings of Birds*, M. K. Hecht, J. H. Ostrom, G. Viohl, P. Wellnhofer, Eds. (Brönnner and Daentler, Eichstätt, Germany, 1984), pp. 251–260.
  17. F. A. Jenkins, *Am. J. Sci.* **293-A**, 253 (1993); S. A. Poore, A. Sánchez-Haiman, G. E. Goslow Jr., *Nature* **387**, 799 (1997).
  18. F. E. Novas and P. F. Puerta, *Nature* **387**, 390 (1997).
  19. J. H. Ostrom, *Peabody Mus. Bull.* **30**, 1 (1969).
  20. P. J. Currie, *J. Vertebr. Paleontol.* **7**, 72 (1987); P. J. Currie and X. Zhao, *Can. J. Earth Sci.* **30**, 2231 (1993).
  21. Morphological information from *Rahona* was combined with that of six bird and eight maniraptoran taxa into a 113-character matrix and analyzed with the PAUP and MacClade programs. Characters were unordered and unweighted, and trees were optimized with the use of delayed transformations. Tree statistics are as follows: The most parsimonious tree shown in Fig. 5A is 228 steps; consistency index (CI) = 0.579, homoplasy index (HI) = 0.421, retention index (RI) = 0.712. The tree shown in Fig. 5B is 229 steps; CI = 0.576, HI = 0.424, RI = 0.709. The character matrix and character list for this phylogenetic analysis are available at [www.sciencemag.org/feature/data/972697.shl](http://www.sciencemag.org/feature/data/972697.shl).
  22. The three forelimb elements of *Rahona* were found either next to or touching the hind portion of the skeleton (Fig. 1B). Because they were not in direct articulation with the rear of the animal, we recognize the possibility, albeit remote in our opinion, that they do not belong to the same individual or taxon. Although material of more derived avians was found elsewhere in the quarry, with the exception of one articulated partial tibiotarsus-tarsometatarsus (14) all avian material occurred as widely scattered, isolated elements. The only articulated skeleton found anywhere in the quarry is that of *Rahona*. Because of the taphonomic distribution of bone in the quarry and the juxtaposition of these forelimb elements with the rear portion of the skeleton, we believe they belong to the same specimen and are confident in assigning them to *Rahona*. Nevertheless, to test the effect of an erroneous association, the phylogenetic analysis was run with two data sets, one including and one excluding forelimb elements for *Rahona*. Each data set resulted in two most parsimonious trees; the ambiguity in these trees was due to the switching of the positions of the theropod taxa Oviraptoridae and Ornithomimidae. The topology of taxa within Aves was consistent across all four most parsimonious trees, with *Rahona* firmly nested within this clade.
  23. J. H. Ostrom, *The Beginnings of Birds*, M. K. Hecht, J. H. Ostrom, G. Viohl, P. Wellnhofer, Eds. (Brönnner and Daentler, Eichstätt, Germany, 1984), pp. 161–176; L. Hou, L. D. Martin, Z. Zhou, A. Feduccia, *Science* **274**, 1164 (1996); N. Bonde, in *The Continental Jurassic*, M. Morales, Ed. (Museum of Northern Arizona, Flagstaff, AZ, 1996), pp. 193–199.
  24. It cannot be ascertained whether *Archaeopteryx* possesses hyposphene-hypantra articulations. Among more derived birds, only the alvarezsaurid *Patagonykus* retains this character.
  25. The foot of *Unenlagia* is not known. However, it has been suggested that *Archaeopteryx* retains vestiges of an enlarged, hyperextendible, second pedal digit and claw. This observation was first advanced by J. Gauthier (3) and more recently revived by G. Paul [Programs and Abstracts, Society of Avian Paleontology and Evolution (Washington, DC, 1996), p. 15].
  26. We thank B. Rakotosamimanana, P. Wright, B. Andriamihaja, the staff of the Institute for the Conservation of Tropical Environments, the people of Berivotra, and all expedition members for their help; and L. Witmer, J. Clark, and an anonymous reviewer for discussions and critiques. D. Varricchio, J. Clark, M. Norell, H. Osmólska, and P. Wellnhofer provided valuable information on theropods and *Archaeopteryx*. *Rahona* was prepared by V. Heisey and photographed by M. Stewart and F. E. Grine (with a scanning electron microscope), and figures were drawn by L. Betti-Nash and C.A.F. This work was supported by grants from NSF and The Dinosaur Society (to C.A.F., S.D.S., and D.W.K.) and the J. S. Guggenheim Foundation and F. Chapman Memorial Fund (to L.M.C.).
- 9 January 1998; accepted 5 February 1998

## Age and Origin of Carlsbad Cavern and Related Caves from $^{40}\text{Ar}/^{39}\text{Ar}$ of Alunite

Victor J. Polyak,\* William C. McIntosh,\* Necip Güven, Paula Provencio

$^{40}\text{Ar}/^{39}\text{Ar}$  dating of fine-grained alunite that formed during cave genesis provides ages of formation for the Big Room level of Carlsbad Cavern [4.0 to 3.9 million years ago (Ma)], the upper level of Lechuguilla Cave (6.0 to 5.7 Ma), and three other hypogene caves (11.3 to 6.0 Ma) in the Guadalupe Mountains of New Mexico. Alunite ages increase and are strongly correlative with cave elevations, which indicates an 1100-meter decline in the water table, apparently related to tectonic uplift and tilting, from 11.3 Ma to the present.  $^{40}\text{Ar}/^{39}\text{Ar}$  dating studies of the hypogene caves have the potential to help resolve late Cenozoic climatic, speleologic, and tectonic questions.

Carlsbad Cavern and Lechuguilla Cave are world renowned for their size, geology, and mineral decorations. These and other related caves are located in the Permian Capitan Limestone, Goat Seep Dolomite, and associated backreef carbonate rocks in the Guadalupe Mountains of southeastern New Mexico and West Texas (1) (Fig. 1). Carlsbad, Lechuguilla, and other major caves of the Guadalupe Mountains formed partly, if not largely, by sulfuric acid dissolution (2–4) rather than solely by carbonic acid dissolution as was initially thought (5). Caves formed by ascending hydrothermal or sulfuric acid-bearing waters are termed hypogene (6–8). Hypogene caves represent at least 10% of the 300+ (9) caves in the Guadalupe Mountains; these are generally the larger caves. Some hypogene caves in the Carlsbad area contain small amounts of alunite, a potassium-bearing aluminum sulfate, which is a by-product of cave genesis (10). Alunite has been used for K-Ar and

$^{40}\text{Ar}/^{39}\text{Ar}$  dating of hypogene and supergene hydrothermal ore deposits (11) and supergene paleoweathering sequences (12). Here, we use alunite to determine the absolute age of formation of Carlsbad Cavern and other related hypogene caves. Previously, ages of these (13) or any other dissolution caves could be estimated only by dating detrital sediments and carbonate precipitates, which establish only the earliest ages of calcite or clastic deposition in the caves.

Alunite is present in Carlsbad Cavern and related caves in floor deposits and wall residues and most commonly within pockets of altered bedrock or solution cavity fillings (10), which may represent paleokarst cavities. Alunite and hydrated halloysite are products of the reaction of acidic cave-forming waters with clays such as montmorillonite, illite, dickite, and kaolinite that occur as detrital components of cavity fillings or in scarce thin Permian clay beds. The Green Clay Room in Carlsbad Cavern presents the most convincing evidence of alteration by sulfuric acid of green montmorillonite-rich sediments that fill solution cavities; white reaction rims around these cavity fillings consist of alunite and hydrated halloysite (Fig. 2A). In Endless Cave, pods of white alunite and hydrated halloysite at the base of a 10-cm-thick Permian clay bed also provide

V. J. Polyak and N. Güven, Department of Geosciences, Texas Tech University, Lubbock, TX 79409–1053, USA. W. C. McIntosh, New Mexico Geochronology Research Laboratory, New Mexico Institute of Mining and Technology, Socorro, NM 87801–4796, USA. P. Provencio, Sandia National Laboratories, Albuquerque, NM 87185, USA.

\*To whom correspondence should be addressed. E-mail: [aqvjp@ttuvm1.ttu.edu](mailto:aqvjp@ttuvm1.ttu.edu) and [mcintosh@nmt.edu](mailto:mcintosh@nmt.edu)